Exploring the regulation of human neural precursor cell differentiation using arrays of signaling microenvironments

Yoav Soen[1],*, Akiko Mori[2], Theo D Palmer[2],* and Patrick O Brown[1,3]

[1] Department of Biochemistry, Stanford University, Stanford, CA, USA, [2] Department of Neurosurgery, Stanford University, Stanford, CA, USA and [3] Howard Hughes Medical Institute, Stanford University, CA, USA
* Corresponding authors. Y Soen, Department of Biochemistry, Stanford University, 279 Campus Dr, Beckman Center B439, Stanford, CA 94305-5307, USA.
Tel.: + 1 650 723 6902; Fax: + 1 650 725 7811; E-mail: yoavs@stanford.edu or TD Palmer, Department of Neurosurgery, Stanford University, 1201 Welch Rd, MSLS P309, Stanford, CA 94305-5307, USA. Tel.: + 1 650 723 9306; Fax: + 1 650 736 1949; E-mail: tpalmer@stanford.edu

Cells of a developing embryo integrate a complex array of local and long-range signals that act in concert with cell-intrinsic determinants to influence developmental decisions. To systematically investigate the effects of molecular microenvironments on cell fate decisions, we developed an experimental method based on parallel exposure of cells to diverse combinations of extracellular signals followed by quantitative, multi-parameter analysis of cellular responses. Primary human neural precursor cells were captured and cultured on printed microenvironment arrays composed of mixtures of extracellular matrix components, morphogens, and other signaling proteins. Quantitative single cell analysis revealed striking effects of some of these signals on the extent and direction of differentiation. We found that Wnt and Notch co-stimulation could maintain the cells in an undifferentiated-like, proliferative state, whereas bone morphogenetic protein 4 induced an 'indeterminate' differentiation phenotype characterized by simultaneous expression of glial and neuronal markers. Multi-parameter analysis of responses to conflicting signals revealed interactions more complex than previously envisaged including dominance relations that may reflect a cell-intrinsic system for robust specification of responses in complex microenvironments.

Introduction

The development of the nervous system depends on spatially and temporally programmed differentiation of multi-potent cells into specific neurons and glial cells. The developmental competence of these precursor cells makes them attractive targets for studying factors and mechanisms that regulate brain development. Moreover, understanding how their differentiation can be regulated is critical for realizing their potential for regenerative medicine. Considerable attention has been therefore devoted to uncovering cell autonomous mechanisms and extrinsic factors that orchestrate determination and differentiation of multi-potent precursors of the central and peripheral nervous system (Morrison *et al*, 1997; Edlund and Jessell, 1999; Jessell, 2000; Anderson, 2001; Bertrand *et al*, 2002; Sauvageot and Stiles, 2002; Ross *et al*, 2003; Sun *et al*, 2003). In the developing nervous system, as in other developmental systems, soluble signals and cell–cell interactions participate in the induction of specific cell lineages. For example, both CNTF and Notch signaling instructively promote astrocytic differentiation in the central nervous system (Johe *et al*, 1996; Ge *et al*, 2002). Bone

morphogenic proteins (BMPs), Neuregulin-1, and TGF$_\beta$ instructively promote differentiation into neural crest autonomic neurons, Schwann cells, and smooth muscle, respectively (Shah *et al*, 1994, 1996). The responses to these signals depend on the identity and state of the responding cells. For example, BMPs can enhance either neurogenesis or glial differentiation depending on the developmental age of the precursors (Gross *et al*, 1996; Li *et al*, 1998; Temple, 2001) and the expression of pro-neural, basic helix–loop–helix transcription factors (Sun *et al*, 2001). The cell context dependency of the response and its complicated inter-relations with external stimulation present a challenge for systematic investigation of the role of extrinsic signals in cell fate determination. Consequently, despite remarkable progress in elucidating individual pathways and cell-intrinsic factors, we are still a long way from an integrative understanding of how these pathways interact with one another and with cell-intrinsic determinants to specify cellular fate and function.

To investigate the influence of combinatorial signaling on neural specification and differentiation, we developed an experimental paradigm that is based on parallel, *in vitro* exposure of neural precursor cells to a diverse array of defined

extracellular signals presented individually and in combinations. Prolonged exposure to these signals was followed by high-throughput quantitative analysis of multiple phenotypic outcomes at single cell resolution. Bi-potent human neural precursors, capable of differentiating into neurons or glial cells, were captured on printed microarrays of extracellular matrix (ECM) components and recombinant proteins, and then allowed to differentiate. Using this approach, we have identified combinations of molecular signals that influence the balance between differentiating neural and glial cells. The 44 signaling combinations that we analyzed could be segregated into four main groups based on their characteristic effects: (1) combinations that promoted neurogenesis, (2) combinations that promoted gliogenesis, (3) combinations that prevented both, and (4) combinations that elevated both neural and glial markers in the same cell, thus establishing an indeterminate differentiation phenotype. Analysis of responses to pairs of individual signals revealed a complex spectrum of responses to contrasting signals, which may have important implications for cell fate specification in a complex signaling microenvironments.

Results

Human cortical precursor model

Bi-potent neural precursor cells were derived from whole cortex of a 22-week human fetus (Palmer *et al*, 2001; Schwartz *et al*, 2003). Rapidly dividing cells were propagated as monolayer cultures on fibronectin (Fn)-coated dishes in serum-free, stem-cell growth-promoting medium, containing EGF, bFGF, and PDGF-AB. When these cells are plated onto a laminin (Ln) substrate in serum-containing medium supplemented with all-*trans* retinoic acid (RA) and the neurotrophic factors NT3 and BDNF, they differentiate into mixed populations composed of neurons and glia (as determined by TUJ1 and GFAP staining) (Palmer *et al*, 2001). In this earlier work, we had found that abrupt withdrawal of growth factors led to dramatic cell death and that the combination of neurotrophic factors and serum provided a baseline survival-promoting environment that allowed exit from cell cycle and efficient differentiation into both neurons and glia. For the present work, we found that the elimination of serum from this differentiation cocktail gave rise to a similar lineage balance without compromising cell viability and provided a more defined medium within which the effects of additional signals could be determined. The balance between neurons and glia produced on a Ln substrate in this medium (75–80% neurons and 20–25% glia) was used as a point of reference, relative to which the effects of additional factors were compared.

Using microenvironment arrays to study control of differentiation

We used a non-contact arrayer (*BCA arrayer*, Perkin-Elmer) to print mixtures of ECM components and putative signaling factors on a glass surface, thereby creating an array of immobilized 'molecular microenvironments', each comprising a defined combination of signaling molecules (Figure 1A). This protein microenvironment-based approach was similar to
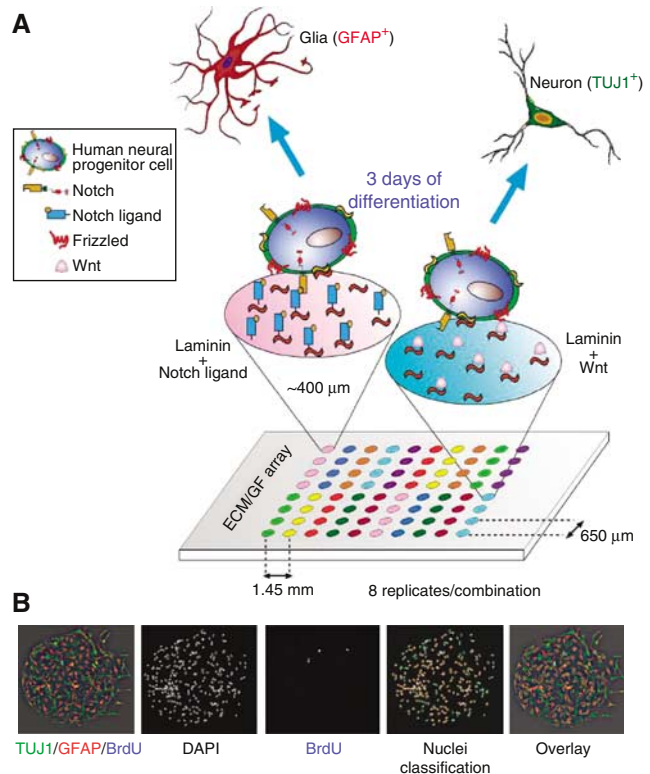

Figure 1 (**A**) Schematics of a molecular microenvironment array experiment. Arrays of pre-mixed combinations of signaling molecules were printed using a non-contact, piezoelectric arrayer. Each spot typically included a combination of Ln and one or more recombinant proteins that were previously implicated in cell fate decision processes. Each combination was printed in two separate groups of four replicates. Bi-potent human neural precursors were captured onto the printed spots by adherence to the Ln. Thereafter, the cells were cultured on the array under defined, differentiation-promoting conditions for about 3 days. Differentiation and proliferation responses to each microenvironment were analyzed by immunostaining with TUJ1, GFAP, and BrdU. (**B**) A basic feature extraction example. Arrays were imaged with four wavelengths using automated fluorescent microscopy. Cell- and image-based information were extracted from each image using an analysis script that measured multiple phenotypes from each cell and computed ensemble average phenotypes. All the nuclei within a spot were detected using the DAPI channel and each nucleus was defined as an object representing a cell. Subsequent measurements were performed with respect to each nucleus and were associated with the corresponding cell. Perinuclear cytoplasmic region was defined by expanding a narrow ring of specified width (0.55 μm) around each nucleus. Cell fate and extent of differentiation were evaluated by measuring TUJ1 and GFAP intensities within the perinuclear ring. Proliferating cells were identified based on intranuclear BrdU threshold crossing. Green and orange circles indicate non-proliferating neuron-like and glial-like cells, respectively (right panel). Blue and white circles correspond, respectively, to proliferating neuron-like and glial-like cells.

that previously used to investigate the specificity and responses of T cells to diverse molecular ligands (Soen *et al*, 2003; Chen *et al*, 2005). To facilitate cell capture, each of the printed combinations typically included one ECM component or a cell adhesion molecule (CAM). These were pre-mixed with one or more recombinant proteins to form defined combinations of signaling molecules, and printed in multiple replicates onto aldehyde-derivatized slides. To allow collection of reliable cellular statistics and maintain good cell viability, each mixture was dispensed in 10 sequential droplets to form an individual spot of about 400 μm in diameter, which sufficed

to capture a few hundreds cells per spot. Printing in replicates further facilitated assessment of the statistical significance of the results by comparing the variation among ostensibly identical spots to the variation among non-identical spots. Replicate spots were printed in two groups of four replicates with 0.65 mm of space between each spot. Non-identical, neighboring microenvironments were separated by 1.45 mm. To evaluate and partially compensate for potential crosstalk between cells on different microenvironments via locally secreted diffusible signals, we printed each group of replicates in two different neighborhoods of printed signals.

Human neural precursor cells were dissociated non-enzymatically (to maintain the integrity of their cell surface receptors) and incubated on the array for 8 min at 37°C and 5% CO_2. The cells were immobilized on the spots by attachment to the printed ECMs or CAMs, and unbound cells between spots were removed by washing in DMEM. We found that a plating density of 400 000 cells/ml was suitable for capturing a sufficient number of cells per spot (between 100 and 400 cells/spot). At higher cell densities, the spots became overpopulated and the distinctive effects of each microenvironment were less apparent. Following cell capture on the microenvironments, the arrays were cultured in differentiation medium (DMEM/F12/BIT/NT3/BDNF/RA) for periods ranging from 1 to 4 days. To prevent microbial growth, medium was supplemented with penicillin, streptomycin, and fungizone.

We tested two array formulations. The first examined different ECM components and CAMs (cadherins, ICAM, VCAM, NCAM, and ephrin A1). Most of these ECMs and CAMs were pre-mixed with recombinant proteins that were previously implicated in regulation of differentiation. The second set of arrays focused on 44 selected combinations of signaling molecules, all containing Ln as a common ECM background. Both ECM components and CAMs were capable of mediating cell capture. However, the CAMs were not compatible with long-term culturing; within a few hours, cells that were initially captured on CAM-containing spots aggregated into clumps and finally detached from the spots (usually within 2 days). In addition, there was typically no binding to spots composed solely of signaling molecules without an ECM component or a CAM. The ECM components Ln, Fn, vitronectin (Vn), and matrigel were all suitable for long-term culturing (Supplementary Figure S2). However, on Fn-containing spots, the cells favored cell–cell versus cell–substrate interactions; they formed three-dimensional, web-like structures of intermingled cells that significantly limited the ability to monitor the fate of individual cells (Supplementary Figure S2C). In contrast, cells that were bound to Ln- (Supplementary Figure S2A), Vn- (Supplementary Figure S2B), and matrigel-containing mixtures (not shown) spread out in a monolayer on the surface of the spots and could be individually assayed with a set of molecular markers.

To examine the effects of the various signal/ECM combinations on cell specification and differentiation, the cells were fixed at the end of the differentiation period and stained with fluorescent antibodies against neural and glial differentiation markers (TUJ1 and GFAP, respectively). BrdU labeling and DAPI staining were used to measure cell proliferation and to define the location and morphology of the nuclei, respectively.

Following immunostaining, each array was uniformly imaged using automated fluorescence microscopy (*ImageXpress*, Axon Instruments) (Figure 1B). Images were automatically annotated and stored in an image database. Cellular phenotypes were measured using a feature extraction script that received images of spots as inputs, identified the cells in the spots, performed multiple measurements on each cell, and computed ensemble average phenotypes by averaging over all the cells in a given spot and subsequently, over spot replicates. To perform the measurements on individual cells, we identified cell nuclei by using a segmentation algorithm applied to the DAPI channel. Nuclear and cytoplasmic regions of each cell were operationally defined as the nucleus interior and a narrow ring surrounding it, respectively. We used background-subtracted TUJ1 and GFAP fluorescent-antibody staining intensities inside the perinuclear ring to classify the cells as neurons or glia, respectively, and to evaluate the extent of differentiation in both lineages. We measured nuclear morphology and proliferation by using DAPI and BrdU intranucleus staining, respectively.

Specific molecular signals in microenvironment arrays differentially affect differentiation of neural precursors. Analysis of the patterns of immunofluorescent staining for GFAP and TUJ1 revealed dramatic, microenvironment-dependent differences in the balance between GFAP (red)- and TUJ1 (green)-stained cells (Figure 2A) along with differences in cellular morphology and arrangement (Figure 2B). We used the GFAP and TUJ1 staining intensities to define quantitative measures of differentiation toward glial or neuronal fates, respectively. On spots consisting of Ln alone (Figure 2, upper left), differentiation was biased toward a neuronal fate, with more than 70% of cells positive for TUJ1 after 3 days. Exposure of the same population of precursor cells to microenvironments containing the Notch ligands rrJagged-1 and rhDLL-4 increased the fraction of cells that differentiated into $GFAP^+$ (presumed glial) cells in a dose-dependent manner. Interestingly, the Notch ligands were less effective without immobilization; incubation with soluble Jagged-1 and DLL-4 at concentrations as high as 5 µg/ml had no significant effect on the balance between $GFAP^+$ and $TUJ1^+$ cells when measured in traditional multi-well assays following the same baseline differentiation condition (Supplementary Figure S3). Other gliogenic factors such as CNTF (Figure 2, bottom right), TGF_β (bottom left), and BMP-4 (third row to the right) also induced a shift in the differentiation outcome toward glial (GFAP-positive) cells. In some cases, the combination of two gliogenic signals (such as Jagged-1 and CNTF) further increased the relative proportion of cells that differentiated into glia ($GFAP^+$). Given the propensity of these precursor cells to differentiate into neurons in the reference microenvironment (Ln alone), neurogenic factors were harder to identify. Nevertheless, we found that Wnt-3A had a neurogenic effect, manifested by a significant reduction in the ratio of $GFAP^+$ to $TUJ1^+$ cells relative to that seen on the Ln-only microenvironment.

We investigated potential paracrine interactions between cells in neighboring microenvironments (owing to secretion and diffusion of factors from a neighboring spot) by positioning replicates of signaling combinations in different neighborhoods and testing for neighborhood-specific phenotypic
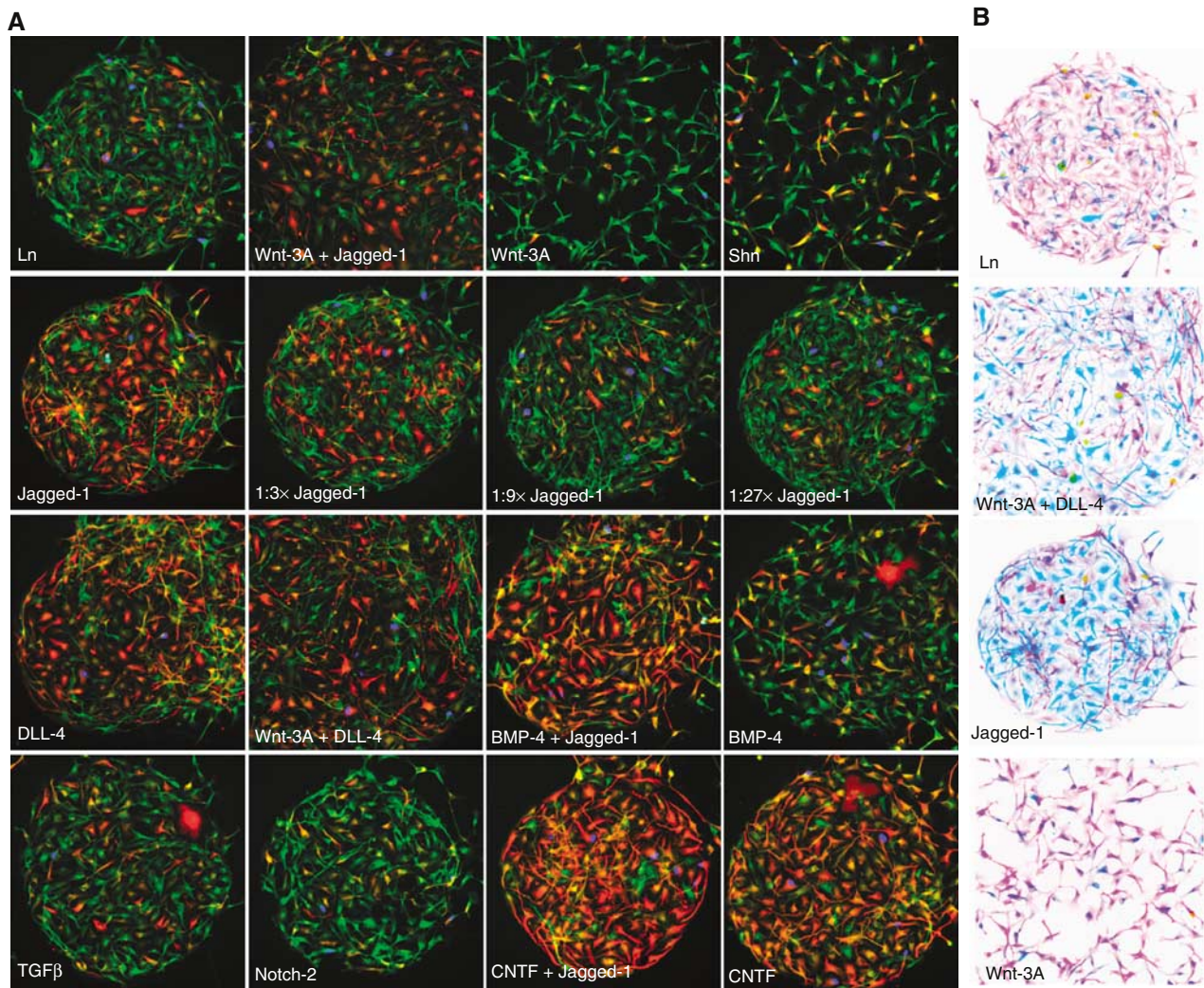
Figure 2 Microenvironment-dependent differentiation and morphology. Human neural precursors were captured and cultured on a printed Ln/ligand array for 70 h under differentiation-promoting conditions. Following the differentiation period, the cells were fixed and counterstained with GFAP (red), BrdU (blue), TUJ1 (green), and DAPI (not shown). (**A**) A small portion of the array with 16 different microenvironments each containing a few hundred cells. The balance between TUJ1 and GFAP staining on the reference Ln spot (top left) was skewed toward preferential expression of the neuronal marker TUJ1. This balance was shifted in a spot-dependent manner by some of the signal-containing spots. In particular, spots containing CNTF (bottom right) and Notch ligands (right panels on the 2nd and 3rd rows) led to a dramatic shift toward increased GFAP proportions, suggesting a gliogenic response to Notch stimulation. Dilution series of Jagged-1 (2nd row panels) revealed dose-dependent response to Notch stimulation. Combination of some gliogenic signals (e.g. Jagged-1 and CNTF) led to further increase in the gliogenic response. A smaller shift toward increased neuronal proportions was observed on Wnt-3A spots. (**B**) Color inverted images demonstrating spot-dependent morphological differences. Cells that were exposed to a combination of Wnt-3A and a Notch ligand (second spot from the top) exhibited longer and more elaborated processes compared to Ln alone (top). Typical spot diameter was 400 μm. Fields of view in all panels are identical in size. Wnt-3A-containing spots consistently larger.

changes. Two groups of four replicates were placed in different neighboring microenvironments and paracrine effects on measured phenotypes were examined by splitting the single cell data into two, neighborhood-based groups followed by an evaluation of the likelihood that the two data sets were drawn from the same distribution. In all tested cases, we found that the sets were statistically indistinguishable (Supplementary Table 3).

Dose response and kinetics with ensemble statistics

We evaluated the response to Notch stimulation as a function of ligand (Jagged-1) concentration (Figure 3A). The fraction of cells that were TUJ1^{high}/GFAP^{low} (% neurons) decreased, whereas the fraction of GFAP^{high}/TUJ1^{low} (% glia) increased monotonically with Jagged-1 concentration. The monotonic dose response and the small variability between replicates (as compared with differences in response between different doses) provide evidence for the reliability and the reproducibility of the spotted protein-based method.

Temporal programs of responses to specific microenvironments were evaluated by performing simultaneous experiments on replicate arrays, each terminated by fixation at a different interval following cell adhesion. Figure 3B contrasts the gliogenic influence of Jagged-1 to that of BMP-4, a protein that we expected would have a similar gliogenic influence but which, instead, had a more complicated effect (see below).

The BMP-4 response reached a plateau within the first 25 h of culture in contrast to the more prolonged and accumulating effects of Jagged-1.

Kinetic profiles of proliferation were obtained by scoring the fraction of cells that became BrdU labeled in the last 13 h of culture in response to different molecular microenvironments (Figure 3C). We found reproducible differences in proliferation responses to different microenvironments. For example, exposure to Wnt-3A resulted in diminished proliferation (compared to Ln) at the 38 h time point (P-value=0.0037)

and enhanced proliferation at the 70 h time point (P-value=0.055). In contrast, Jagged-1 led to a monotonic decrease in proliferation. Unexpectedly, combined exposure to Wnt and Notch ligands resulted in the highest net increase in proliferation, which peaked at 52 h and returned to baseline by 70 h. Owing to the dynamic changes in proliferative activity, we subsequently averaged the proliferation indices over multiple time points to obtain a 'smoothed' relative index of proliferative activity in response to each of the microenvironments.

Single cell (FACS-like) analysis of differentiation

The ability to measure multiple parameters in individual cells allowed heterogeneous responses to be profiled in detail at single cell resolution. To represent the extent of neural and glial differentiation in single cells, we defined a 'differentiation space' spanned by the intensities of the neural and glial reporters, TUJ1 and GFAP, respectively (Figure 4A). In this representation, each cell corresponds to a single coordinate defined by its TUJ1 and GFAP staining intensities. The location of each cell in the plane was used to operationally estimate the direction and extent of its differentiation. Cells within the region that corresponds to medium or high TUJ1 levels and low GFAP intensities (green-boxed region of Figure 4A) were classified as 'neuron-like'; cells with medium or high GFAP and low TUJ1 expression (red-boxed region) were classified as 'glial-like'; cells with low expression of both TUJ1 and GFAP (blue-boxed region) were classified 'undifferentiated-like', and cells with medium to high expression of both proteins (orange box) were said to be in an indeterminate state of differentiation. The ensemble of cells analyzed from all the replicate spots of a given composition yielded a distribution that was characteristic of that particular combination of molecular signals. Figure 4A demonstrates two such distributions, corresponding to the reference (Ln) distribution (pink dots) and a combined exposure to Wnt/Jagged stimulation (light blue dots), respectively. Simultaneous exposure to Wnt-3A and Jagged-1 significantly shifted the distribution toward lower TUJ1 intensities (Figure 4B), suggesting a decrease in neuronal differentiation.

The effects of specific molecular signals on neural precursor cell differentiation were visualized by plotting the distribution of cells with respect to GFAP and TUJ1 immunofluorescence.
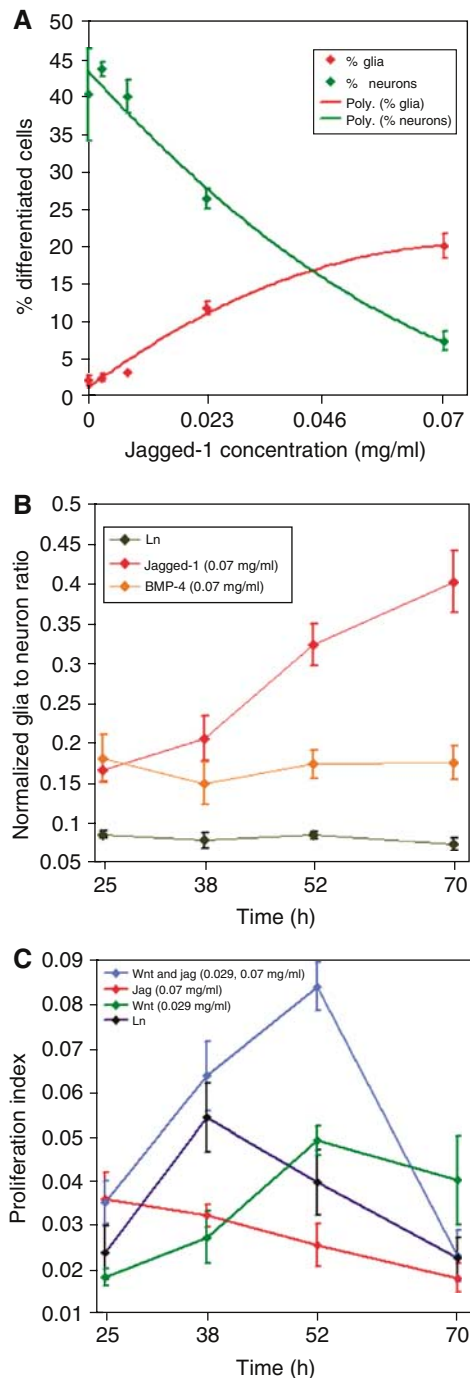

Figure 3 Dose response (A) and kinetic measurements (B, C) on the array. (**A**) Percentiles of differentiated neuron-like cells (green) and glial-like cells (red), as a function of spotted Jagged-1 concentration. The higher the concentration of the Notch ligand, the higher or lower the percentage, respectively, of differentiating glial-like and neuron-like cells. Red and green lines represent polynomial fits. Error bars represent standard errors computed using spot replicates on the same array. (**B**) Differential kinetics of gliogenic responses. Shown are four time points from a time-course experiment conducted in parallel with four arrays that were cultured for 25, 38, 52, and 70 h. Exposure to BMP-4 (orange) and Jagged-1 (red) increased the relative proportions of glia as compared to Ln (black). The BMP-4 response was already at a plateau after 25 h, whereas the response to Jagged-1 stimulation occurred over a significantly longer timescale. (**C**) Differential kinetics of proliferation. Traces of proliferation index in the same time-course experiment revealed dynamic, spot-dependent differences in proliferation responses. Integration over all four time points revealed that co-exposure to Wnt-3A and Jagged-1 (light blue) or DLL-4 (not shown) led to a significant increase in proliferation.
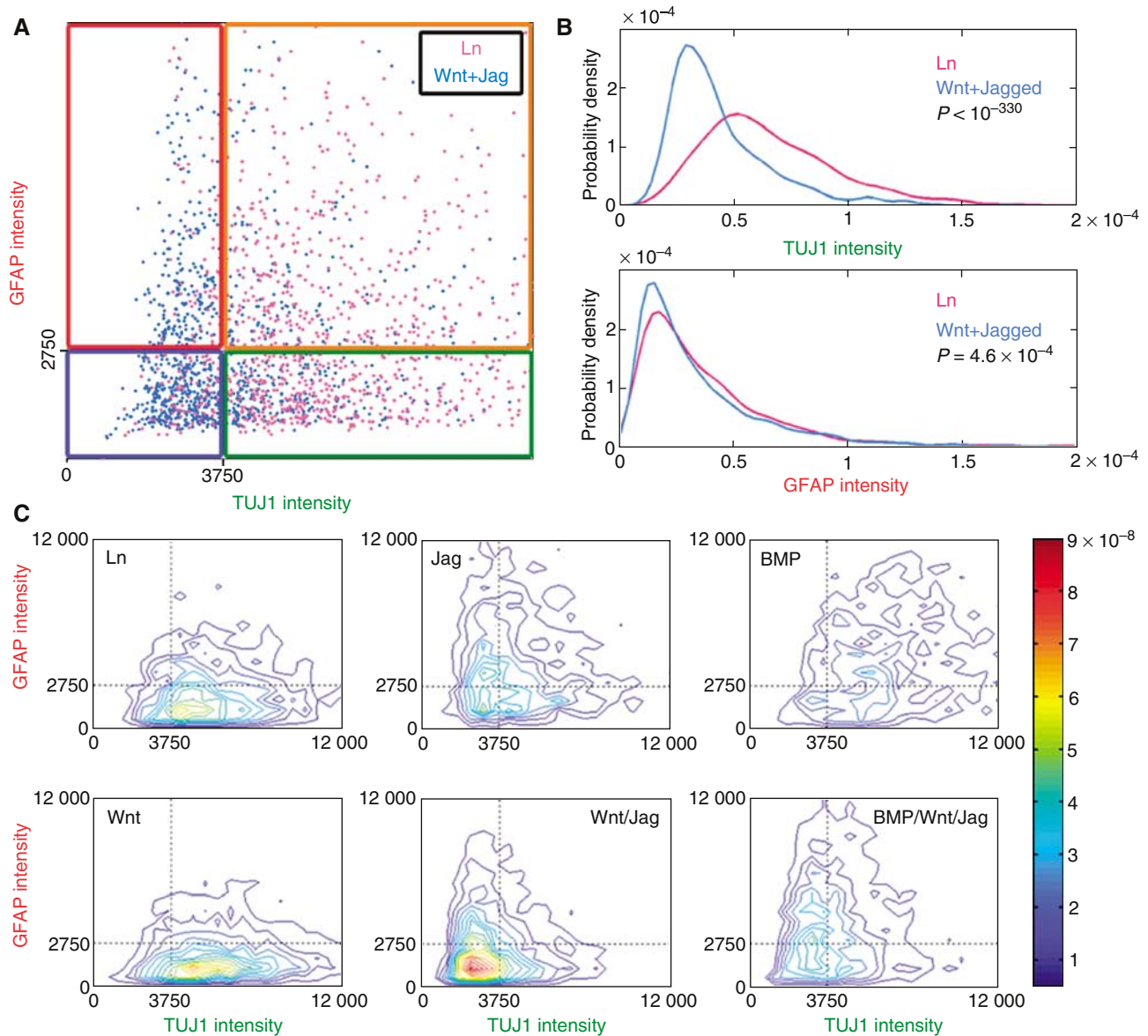
Figure 4 Analysis of differentiation in single cells. (**A**) TUJ1 and GFAP intensities recorded from individual cells were represented by a coordinate in a 'differentiation plane' whose axis was defined by these intensities. The TUJ1-GFAP plane was divided into neural-like (green rectangle), glial-like (red rectangle), undifferentiated-like (blue rectangle), and indeterminate differentiation (orange rectangle). Measurements from all the cells that were exposed to the same signaling combination yielded a distribution that was characteristic to that combination. Shown are two such distributions corresponding to Ln (purple) and Wnt-3A/Jagged-1 (light blue) stimulation. The Wnt-3A/Jagged-1 distribution was shifted toward lower revels of TUJ1 staining intensity, resulting in a marked elevation in the fraction of undifferentiated-like cells (blue rectangle). (**B**) Individual TUJ1 (top) and GFAP (bottom) probability density functions, demonstrating the decrease in TUJ1 intensity values in response to co-exposure to Wnt-3A and Jagged-1. (**C**) Contour plots of the estimated two-dimensional probability density of cells for various stimuli. Note the strong Wnt-3A/Jagged-1-mediated increase in the proportions of undifferentiated-like cells (bottom center) compared to Ln (top left).

Figure 4C displays contour plots of these distributions for six different signaling combinations. The plane was divided into four segments representing undifferentiated-like cells (lower left), glial-like cells (upper left), neuron-like cells (lower right), and indeterminate differentiation (upper right). Compared to Ln alone (top left panel), the Notch ligand, Jagged-1 (top middle), induced an increase in the proportion of cells differentiating into glia and a decrease in the proportion differentiating into neuronal cells. The other Notch ligand, DLL-4, had a very similar effect (not shown). Conversely,

compared to Ln alone, Wnt-3A had a weak neurogenic effect (bottom left panel). The combined exposure to Wnt-3A and Jagged-1 (bottom center) significantly increased the proportion of cells expressing low levels of both TUJ1 and GFAP, suggesting maintenance in an undifferentiated state. Note that the Wnt/Jagged-mediated enrichment of TUJ1^{low}/GFAP^{low} cells was also associated with a net increase in proliferation (Figure 3C), with the most significant enhancement observed after 52 h (*P*-value$=1.2 \times 10^{-4}$). The results are consistent with a model in which Wnt and Notch ligand can act in concert

to promote retention of undifferentiated-like or 'stem-like' characteristics in these neural progenitor cells. In contrast, BMP-4 significantly increased the fraction of TUJ1^{high}/GFAP^{high} cells (top right panel), corresponding to an indeterminate differentiation phenotype, and produced a broader distribution of cells with respect to expression of these molecules (suggesting a more heterogeneous population in terms of the differentiation state). This effect was reproduced in a standard plate assay with soluble BMP-4 (Supplementary Figure S3, bottom right panel). BMP-4 also antagonized the ability of the Wnt/Notch ligand combination to promote an undifferentiated (TUJ1^{low}/GFAP^{low}), proliferative phenotype (Figure 4C, bottom row, middle and right panels).

Global analysis of differentiation

As the differences in response to variations in the molecular microenvironments are complex and multi-dimensional, it may be useful to develop measures of similarity between responses, and tools for visualizing multi-dimensional responses to a variety of signals. To quantify and analyze similarities and differences between differentiation responses to different combinations of molecular signals, we divided the two-dimensional space of TUJ1 and GFAP staining into nine bins defined by low, medium, and high GFAP or TUJ1 staining intensities, and represented the response to each microenvironment with a profile defined by the fraction of cells measured in each of the bins, normalized relative to the corresponding fraction measured on the Ln reference spots on the same array. The set of all normalized profiles formed a 'map' relating diverse signaling combinations to the corresponding differentiation responses. This map can be displayed as a matrix, with rows corresponding to signaling combinations and columns representing normalized fractions of cells. We clustered the rows and columns based on Pearson correlations of the corresponding profiles (Eisen *et al*, 1998) and displayed the results using a color code with red and green pixels representing an increase or decrease in the % of cells within a given bin, relative to Ln (Figure 5). The larger the deviation compared to Ln, the brighter the colors. Empirically, most signal combinations were strongly segregated into one of four main groups, each with a characteristic profile that roughly corresponded to the four main regions of the differentiation space (i.e., the color-labeled regions of Figure 4A scatter plot). Notably, each of the four effect-groups included signaling combinations that had some signals in common. For example, all conditions that increased the proportion of TUJ1^{low}/GFAP^{low} (presumed undifferentiated) cells included both Wnt-3A and a Notch ligand (Figure 5, blue cluster). Many of the differentiation responses, such as the gliogenic-like effects of CNTF and Notch ligands, were consistent with previous reports. None of the responses we observed conflicted with previously published results, suggesting that the spotted arrays provide a reliable tool for evaluating cellular responses to signaling microenvironments.

Interactions among molecular signals

To examine differentiation responses following simultaneous exposure to potentially conflicting signals (e.g. neurogenic and gliogenic signals), we compared the responses to individual signals with responses to the combined signals. We found that combinations of signals often promoted unique responses that can be completely different than anticipated from the effects of single factors. For example, phenotypic responses to signaling with Jagged-1 and Wnt-3A alone were categorized as gliogenic or neurogenic, respectively. However, in combination, these molecules increased the percentages of cells expressing low levels of both TUJ1 and GFAP (Figure 5, bottom right), suggesting an inhibition of differentiation in both lineages. Simultaneous exposure to Wnt-3A and Jagged-1 also increased the size of the nucleus, although Wnt-3A and Jagged-1 individually had little or no effect on the nucleus area (Supplementary Figure S5A, second column).

In some cases, however, the response to one of the signals appeared to dominate over the response to another signal. For example, with respect to the percentage of cells expressing high GFAP but low TUJ1 levels (Figure 5, third column from the right), the response to Jagged-1 predominated over the response to Wnt-3A when the two proteins were both present.

To further examine dominance relationships, we considered all pairs of signaling molecules (e.g. Wnt-3A and Jagged-1). For each pair, we assigned a dominance score with respect to three parameters: the proliferation index, the 'direction' of differentiation defined as the GFAP to TUJ1 intensity ratio, and the 'extent' of differentiation defined as the Euclidean sum of the TUJ1 and GFAP staining intensities. For each parameter, we then computed the absolute value of the deviations between the responses to the individual signals and the responses to simultaneous exposure to both signals. The dominance score was defined as the difference between these absolute deviations, normalized by the response to the combined signals. The dominance relationships between pairs of signals sometimes differ depending on the response parameter measured. With respect to a specific response parameter, however, the response to one of the signals could dominate over the responses to a group of other signals (or combinations of signals). For example, with respect to the direction (but not the extent) of differentiation, the response to Jagged-1 dominated over the response to each of 11 other signaling mixtures (Figure 6). Interestingly, with respect to proliferation, the situation was reversed and the responses to most of the other signals were dominant over Jagged-1. Although their molecular interpretation is far from clear, these reciprocal dominance relationships show that at least for these signaling combinations, the apparent dominance cannot be trivially explained by differences in effective dose.

Discussion

A microarray of microenvironments as a platform for systematic studies of signaling

The remarkable combinatorial diversity of molecular microenvironments in multi-cellular organisms, and the cell type and context dependency of the cellular response present a tremendous challenge as we seek to understand the programs and mechanisms that control cellular behavior and developmental fate. Recent work has demonstrated the use of synthesized biomaterial microarrays (Anderson *et al*, 2004)
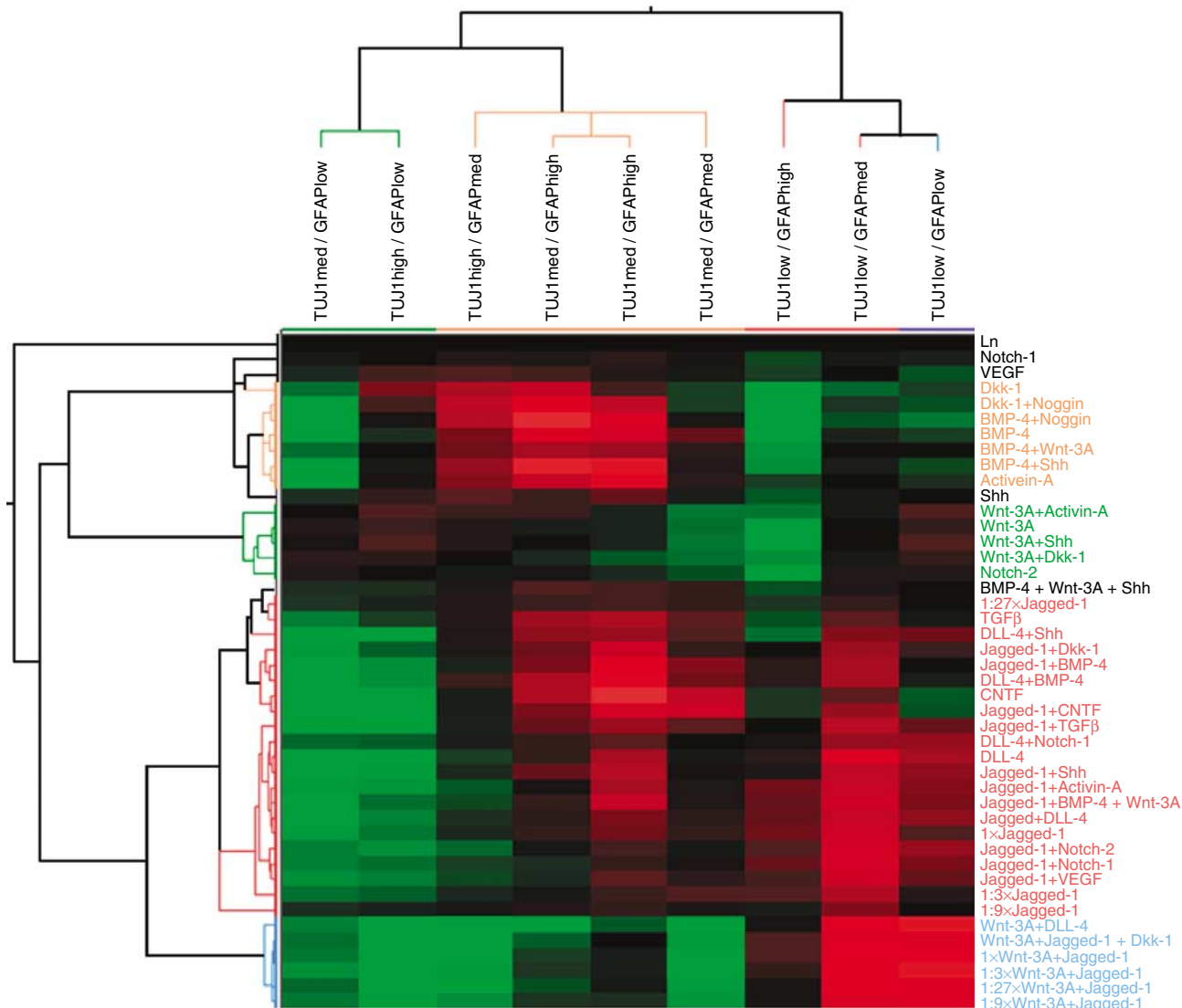
Figure 5 A color-coded map connecting external stimulation (in rows) to differentiation-related phenotypes (columns). Columns display relative fractions of cells measured in each of nine regions of the TUJ1-GFAP 'differentiation plane' representing low, medium, and high staining intensity for each marker. Each row corresponds to a particular signaling microenvironment. Ensemble average fractions of cells were measured in two array experiments, averaged across experiments, and normalized by the corresponding values on spots containing Ln alone. Normalized values were log-transformed and each column was scaled to a unit standard deviation. Red and green colors represent higher and lower than Ln values, respectively. Rows and columns were clustered using Pearson correlation as a similarity metric. Signaling combinations that induced a similar TUJ1-GFAP distribution profile were clustered together, resulting in four main groups of influence: (i) gliogenic-like (red-labeled), (ii) neurogenic-like (green), (iii) undifferentiated-like (light blue), and (iv) indeterminate differentiation (orange).

and ECM microarrays (Flaim *et al*, 2005) for manipulating the behavior of embryonic stem cells. Additional platforms incorporated arrays of printed DNA (Ziauddin and Sabatini, 2001; Wheeler *et al*, 2004) or small molecules (Bailey *et al*, 2004) in cell-based assays. In this study, we found that microarrays of diverse 'molecular microenvironments' — combinations of defined ECM components and signaling proteins — are a practical and useful experimental platform for systematically investigating the responses of cells to molecular signals in their microenvironments. The method allows systematic, reproducible analysis of diverse cellular responses to a diverse array of molecular signaling events in a high-throughput, parallel way that lends itself to quantitative

analysis. Although we focused here on a set of physiological signals and a single ECM protein, this method could readily be expanded to allow the presentation of arbitrary mixtures of purified proteins.

We examined several critical methodological issues. We found that mechanically printed immobilized mixtures of signaling proteins (including proteins that are normally secreted as soluble molecules *in vivo*) are generally functional, and able to induce cellular responses similar to those induced by the molecules in solution. The potential effects of secretion and diffusion of factors from cells on a neighboring spot were evaluated by examining differences between replicates adjacent to different microenvironments. Although in the few
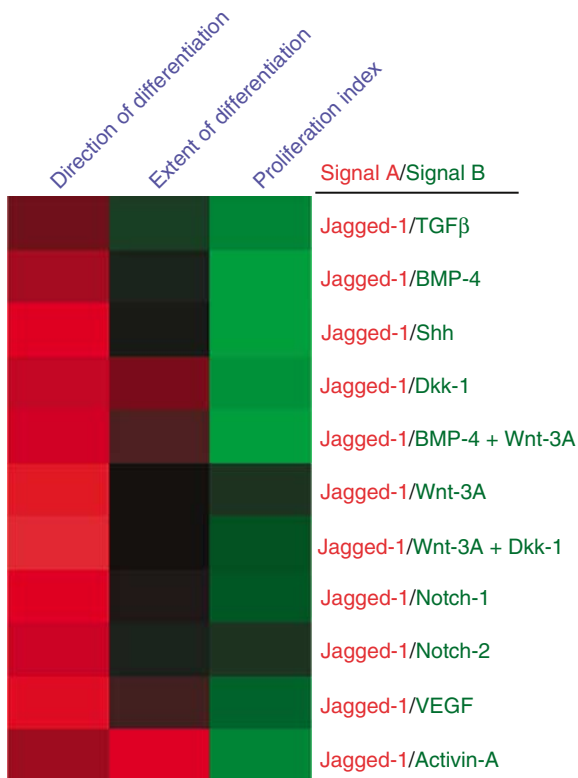
Figure 6 Evaluation of dominance relations between Jagged-1 and other signaling environments with respect to differentiation- and proliferation-related phenotypes. Each row corresponds to a specific signaling pair containing Jagged-1 as one of the signals. Each column denotes a specific phenotype. Direction of differentiation refers to the ratio of GFAP to TUJ1 staining. Extent of differentiation represents the intensity of lineage marker staining, and proliferation index indicates the fraction of BrdU-positive cells. Dominance over a particular phenotype was evaluated based on the difference between the responses to the individual signals and the response to the combined signals. Dominance scores are displayed in a color code with red pixels designating dominance of the response to Jagged-1 and green corresponding to dominance of the response to the other signal (or a combination of signals). The brighter the color, the stronger the dominance. Note the dominance of Jagged-1 response with respect to the direction of differentiation (left column) and the inverse relation with respect to the proliferation index (right column).

tested cases we did not find significant paracrine interactions between neighboring signals, we cannot rule out subtle paracrine effects, nor can we exclude potential crosstalk between signals. Note, however, that by averaging over randomly placed replicates, the potential confounding effect of paracrine interactions can be normalized without compromising the ability to search for neighborhood-dependent anomalies that could reveal crosstalk between signals.

The choice of basal differentiation medium is critical for the efficiency and fidelity of the response to the immobilized factors and to our ability to interpret the results. The studies presented here were performed using culture conditions that favor differentiation of neural precursor cells into neurons. Although this specific design favors detection of signaling combinations that can significantly alter, overcome, or subvert the influence of this neurogenic environment, complementary studies could be carried out using basal conditions that favor glial fates or even undifferentiated growth.

Using this microarray in combination with a uniform, high-throughput imaging and high-resolution feature extraction algorithm allowed us to map a wide range of molecular signal combinations to multiple differentiation-, proliferation-, and morphological-related phenotypes (Figure 5 and Supplementary Figure S5A). By expanding the diversity of molecular markers or cellular phenotypes measured in each assay, we can further extend this map to a wider spectrum of cellular responses.

Implications of ligand immobilization

Although efficient application of growth factors in soluble form has been well documented, experiments with membrane-bound ligands have sometimes yielded different results. In particular, it has been shown that immobilization of Delta-1 (in either monomeric or dimeric form) is required for Notch activation and that the soluble form blocks the activity of the immobilized ligand (Varnum-Finney *et al*, 2000). On the other hand, conditioned medium with soluble Delta-FC (clustered by anti-FC antibody) was shown to inhibit neuronal differentiation of neural crest stem cells (NCSCs) (Morrison *et al*, 2000). Here, we found that secreted and membrane-bound ligands were both active in an immobilized form, whereas soluble versions of monomeric Notch ligands were inactive even at fairly high concentrations (Supplementary Figure S3, middle row). This may be owing to localized concentration effects where ligand concentration in the spots is very high relative to fully solublized proteins. Alternatively, this may be owing to unique attributes of tethered ligands or of their association with the ECM, which may allow them to more efficiently trigger receptor mobilization, clustering, and signal transduction.

Taken together, these results emphasize the importance of ligand presentation effect on its activity, at least in some cellular contexts. Presentation-dependent activity of ligands may have a significant role *in vivo*, where signaling, differentiation, and morphogenetic events often take place in relatively restricted compartments containing signals that are frequently bound to ECM components (e.g. heparan sulfate proteoglycan) or presented on the surface of neighboring cells (e.g. Notch ligands). Arrays of immobilized microenvironments may therefore form an attractive mimic of physiological signaling environments. In addition, they provide a practical tool for studying the implications of immobilization and association of ligands with ECM and/or CAMs.

Instructive influences on the microenvironment microarray

Microenvironment-dependent changes in the balance between GFAP$^+$ and TUJ1$^+$ cells could potentially be attributed to (i) initial, adhesion-dependent cell selection by the spots, (ii) lineage- and signal-specific migration between spots, (iii) signal-dependent amplification and/or death of specific lineages, and (iv) induction by spotted signals. Differential adhesion and selective migration was ruled out for some of the factors (including the Notch ligands, BMP-4, and Wnt-3A) by reproducing the results in a standard multi-well plate assay

where all cells are retained in the well (Supplementary Figure S3). Likewise, selective migration was ruled out by the complete absence of cells between spots throughout the experiment. Selective proliferation is unlikely, as the rates of BrdU incorporation were typically too low (less than 5% of the cells traversing S-phase in a 13 h time period) to account for dramatic shifts in the TUJ1-GFAP balance. For example, the ratio between the numbers of glial and neural cells on CNTF spots increased by about 35% over 13 h, whereas only 3.9% of the cells were cycling during the same period of time, suggesting an inductive rather than selective mechanism. In addition, there was no significant difference in proliferation indices of glial and neural subsets of cells (3.5 ± 1.6 and $4.4 \pm 1.9\%$, respectively). Standard experiments in a multi-well plate format also revealed low and roughly lineage-independent proliferation rates (below 5% of the cells traversing S-phase in a 13 h) in response to immobilized Notch ligands, and soluble BMP-4, Shh, and Wnt-3A (with and without Jagged-1), providing further evidence against selective proliferation. Selective cell death is unlikely to account for variation in relative numbers as the number of cells on the spots did not change dramatically over the course of the experiment (less than 30% variation in cell numbers), nor was cell number variation correlated with specific signal compositions. We are therefore left with differential induction of differentiation by the different molecular microenvironments as the most probable cause of differences in the patterns of TUJ1 and GFAP expression.

TUJ1 and GFAP as surrogates for evaluating differentiation

TUJ1 and GFAP are frequently used as neural and astrocyte differentiation markers, respectively (Park *et al*, 1999; Sun *et al*, 2001; Lie *et al*, 2002; Song *et al*, 2002; van Praag *et al*, 2002; Gajavelli *et al*, 2004). TUJ1 is one of the earliest markers of neuronal commitment in primitive neuroepithelium (Caccamo *et al*, 1989; Lee *et al*, 1990; Easter *et al*, 1993) and GFAP is a developmentally regulated intermediate filament found in the cytoplasm of astrocytes and other types of glial cells, and whose expression in astrocytes increases progressively with differentiation (Pixley and de Vellis, 1984; Wofchuck and Rodnight, 1995; Hogg *et al*, 2004). Although the process of neural and glial differentiation is far too complicated to be fully represented by these two molecular markers, large shifts in the TUJ1-GFAP balance most probably reflect changes in the relative fraction of neurons and glia. TUJ1 and GFAP staining intensities were, therefore, used to lay out an operational framework that would allow us to define differentiation-related phenotypes (such as the 'direction' and 'extent' of differentiation) and compare the responses to diverse stimulations in a more quantitative fashion, capable of capturing non-traditional phenotypes (e.g. the BMP-4 indeterminate phenotype, discussed below) without necessarily relying on arbitrarily chosen thresholds. The conclusions made are, of course, subject to this phenotypic framework and, consequently, the phenotypic influences should be referred to as 'neuron-like', 'glial-like', 'undifferentiated-like', and 'indeterminate differentiation'. Retrospectively, we found that many of

the previously reported influences of these molecular signals were confirmed by this type of analysis, thus validating our strategy as both efficient and predictive.

Response of human neural progenitors to Notch stimulation

The Notch pathway has been implicated in the maintenance of neural stem cell state, inhibition of neural differentiation, and promotion of glial fates (Gaiano *et al*, 2000; Wang and Barres, 2000; Gaiano and Fishell, 2002; Ge *et al*, 2002). Our results provide evidence for these effects in the context of bi-potent human neural progenitors. These effects were eliminated by treating the cells with a soluble form of the Notch inhibitor γ-secretase (DAPT), thereby providing further evidence for the involvement of the canonical Notch pathway in inducing the observed phenotypic changes (A Mori *et al*, unpublished work).

Interaction between Wnt and Notch pathways

The significant elevation of the fraction of TUJ1^{low}/GFAP^{low} cells (Figure 4C, bottom center versus top left) suggests that combined Wnt-3A/Notch signaling promotes maintenance of an undifferentiated-like state. This effect was consistent across experiments and different Wnt-3A/Notch ligand mixtures. Comparison of the responses to Wnt-3A and Notch ligands individually and in combination suggested an underlying mutually antagonistic mechanism (Supplementary Figure S6); in the presence of Wnt-3A, the addition of a Notch ligand leads to an overall decrease in TUJ1 expression and an increase in GFAP expression (Supplementary Figure S6A), suggesting that Notch ligands antagonize the neurogenic-like effect of Wnt-3A. Conversely, in the presence of Jagged-1, the addition of Wnt-3A led to an overall decrease in the expression of both TUJ1 and GFAP (Supplementary Figure S6C), suggesting that Wnt-3A antagonizes the glial-like promoting activity of the Notch pathway, and enhances jagged-1-mediated blocking of neuronal differentiation. The combined effect is a suppression of differentiation toward either lineage. The undifferentiated-like phenotype was also associated with an increase in the average proliferation index (Figures 3C and Supplementary Figure S6A and C) and nucleus area (Supplementary Figures S5A, S6A, and C). Overall, the results are consistent with joint Wnt and Notch signaling acting to oppose differentiation of neural progenitor cells and perhaps promote a self-renewing, undifferentiated state. Notably, a similar role for Wnt and Notch interaction has recently been reported in hematopoietic stem cells (Duncan *et al*, 2005). Perhaps, *in vivo* microenvironments in which cells are exposed to these two ligands provide discrete niches for self-renewal of progenitor cells.

BMP-induced co-expression of neuronal and glial markers

Microenvironments containing BMP-4 on an Ln substrate promoted co-expression of both GFAP and TUJ1 in individual cells, suggesting that there are distinct environments where

the early stages of lineage determination represented by these two markers are not mutually exclusive. This effect was confirmed in a standard multi-well plate format with soluble BMP-4. TUJ1^{high}/GFAP^{high} cells do not correspond to a well-characterized cell type or differentiation intermediate. We do not know whether this indeterminate state reflects an artificial scenario wherein an ectopic presentation of a signal drives a developmentally irrelevant response, or a normally transient developmental intermediate whose eventual fate depends on additional factors. Previous work has identified two stage-dependent contexts in which a BMP signal gives rise to totally different developmental outcomes. In mouse and rat, BMPs have been reported to enhance either neural or glial differentiation, depending on the developmental stage. BMPs promote neural differentiation of early-stage (mouse E13) neural progenitor cells (Li *et al*, 1998) as well as astrocytic fate in late precursors (mouse E17) (Gross *et al*, 1996). In addition, the proneural gene Ngn1 can convert BMP from a glial-inducing cue to a neural-promoting factor (Sun *et al*, 2001). In its absence, BMP-7 induces glial differentiation via the co-activating complex CBP/p300/phosphorylated-Smad1. Ngn1 is highly expressed at an early stage of cortical development ($\sim$E13 in mouse and rat) and is downregulated at a later stage ($\sim$E17–E18). Perhaps in between the neurogenic and gliogenic stages, intermediate levels of proneural genes permit BMP-mediated activation of both pathways in the same cell. The neurogenic phase in human brain peaks at about week 12 and extends between the first and fourth months of gestation, whereas gliogenesis starts during the third trimester and peaks after birth. The cells used in this study were isolated from a 22-week fetus, which might therefore correspond to an intermediate developmental stage.

Analysis of signaling influences in a single cellular model

Responses of neural precursors to external challenge are known to be highly age-, prep-, and culture-dependent. Consequently, the specific kinetics or amplitude of cellular responses to specific signals can vary if one were to compare other cell isolates or cells from different ages of development. We eliminated these sources of variations by consolidating all the external challenges into a given cellular model, thus allowing a direct, integrative analysis of responses to diverse signaling microenvironments (i.e. without relying on inferences from other cellular models). Extending this approach to additional cellular models should allow comprehensive examination of the variation of cellular competence as a function of developmental age, history of past treatments, and other factors. It may also reveal model-independent influences shared by different human neural precursor cultures.

Processing of conflicting signals

In vivo, cells are frequently exposed simultaneously to several instructive signals, which individually could elicit different or even conflicting responses. The ability to respond in a robust manner to potentially conflicting signals may be a significant

element of cell signaling systems. Cortical precursors and NCSCs have been previously shown to process neurogenic and gliogenic cues in a hierarchical manner, with one signal dominating over the other (Shah and Anderson, 1997; Park *et al*, 1999; Morrison *et al*, 2000); bi-potent rat E14 neuroepithelial cells adopted a neural fate in response to PDGF despite the presence of CNTF, which would otherwise instruct a glial fate (Park *et al*, 1999). Similarly, induction of a gliogenic fate in response to Notch signaling was shown to be dominant over the neurogenic activity of BMP-2 in E14.5 rat NCSCs. By examining interactions between multiple pairs of signals, we found that the response to one of the signaling factors, Jagged-1, was dominant over the response to a variety of signals, with respect to the direction of differentiation (measured by the ratio between GFAP and TUJ1 expression in the same cell). Although this is consistent with the idea that Notch signaling provides robust specification of a glial cell fate in the presence of conflicting signals, further investigation is required in order to examine the sensitivity of this apparent dominance to variations in signal dosage. In addition, it is important to note that 'dominance' may not extend to all phenotypic parameters. For example, we found that although Jagged-1 tended to dominate over many signals with respect to its gliogenic influence, the mitogenic influences of co-signaling molecules were not impaired by Jagged 1, which alone yielded relatively low proliferative activity (Figure 6). This segregation of influences and signaling interactions (or lack of interactions) indicates how elegantly the cell-intrinsic parsing of complex environments can yield carefully balanced instructive and selective alterations in cellular outputs. Detailed information regarding dominance relations with respect to specific phenotypes may prove useful for designing molecular approaches for programming complicated cellular responses by combining signals that are synergistic, dominant, mutually antagonistic, or non-interacting with respect to specific desired responses.

Ex vivo culturing and analysis of rare cells

The tremendous potential of the use of *ex vivo* conditions to study mammalian cell biology has yet to be realized, largely owing to the difficulty of defining culture conditions that allow cells to preserve *in vivo*-like characteristics and behavior. The microarray approach provides an efficient way to explore a variety of defined culture conditions and to dissect cellular responses to diverse molecular signals. This approach is particularly valuable in many interesting cases in which the number of cells available for *ex vivo* investigation is severely limited. For example, the number of cancer stem cells isolated from a tumor is often below 10^5 (Al-Hajj *et al*, 2003). Such a limited number of cells does not suffice for systematic functional studies with standard methods, but may be amenable to systematic study using microenvironment arrays, which couple densely packed molecular microenvironments with high-throughput, quantitative analysis of cellular responses at single cell resolution. This approach should lead to significant progress toward understanding the mechanisms by which the molecular composition of the cell's microenvironment shapes its behavior and developmental fate.

Materials and methods

Cell derivation and culture

Post-mortem tissue of a 22 weeks-of-gestation premature infant with a Krabbe disease was obtained from NHNSCR with informed consent procedure and prepared essentially as previously described (Palmer *et al*, 2001). Whole cortex tissue was dissected, minced with blades, and treated for 40 min at 37°C (occasional gentle mixing) with enzymatic solution containing 2.5 U/ml papain, 250 U/ml DNase I, and 1 U/ml dispase II. Following a wash with 10% FBS/DMEM, the tissue was triturated with gentle pipetting and centrifuged three times. Dissociated cells were subsequently plated on Fn-coated dishes using the same medium. The next day, one-fourth of the medium was replaced with serum-free growth medium containing DMEM/F12 (Mediatech Inc.), 10% BIT9500 solution (StemCell Technologies), and 20 ng/ml each of EGF (Sigma), bFGF (Peprotech), and PDGF-AB (Peprotech). Thereafter, half the medium was changed every other day, and the cells were trypsinized (0.25%) and passaged upon reaching about 90% confluency.

Array preparation

Defined combinations of mouse Ln (Invitrogen) and recombinant signaling molecules from various species (R&D Systems; Supplementary Table 1) were pre-mixed and prepared in a 384-well plate (MJ Research) at 14 μl/well. Glycerol was added to each combination (final concentration of 2%). The pre-mixed samples were dispensed onto aldehyde-derivatized slides (*SuperAldehyde*, Telechem International Inc.) using a robotic, non-contact piezzo electric arrayer (*BCA arrayer*, Perkin-Elmer). Each sample was represented by two groups of four replicate spots. Each spot was dispensed in 10 drops of ~0.45 nl, resulting in spot diameter of 350–450 μm (except for Wnt-containing spots, which were consistently larger). Inter- and intra-replicate distances were set to 1.45 and 0.65 mm, respectively. Following printing, arrays were transferred to a sealed box and stored at 4°C until used. Array boundaries were marked with a diamond pen. Arrays were functional for at least 3 months following printing. One hour prior to initial incubation with cells, arrays were placed in 10 cm dishes, and blocked for 45 min (at RT) with 2% BSA and 1.5 × of penicillin, streptomycin, and fungizone in calcium and magnesium free (CMF) PBS. Blocked arrays were washed 2 × with CMF PBS and transferred to a dry dish 15 min prior to cell plating.

Array culturing procedure

Cells were dissociated non-enzymatically by washing with 5 ml of pre-warmed CMF PBS followed by 5–10 min incubation with 4 ml of pre-warmed enzyme-free dissociation solution (Specialty Media). Cells were triturated with gentle pipetting and spun down (without quenching) for 5 min at 1000 r.p.m. Cells were re-suspended at 0.4×10^6/ml using pre-warmed DMEM/F12 and 10% BIT. Suspended cells were incubated on the array for 8 min at 37°C and 5% CO_2. Single cell populations were captured on the spots by adherence to the printed ECM components and/or CAMs. To remove unbound cells between spots, arrays were held by sterilized forceps and washed in a large chamber with pre-warmed DMEM. To promote differentiation, the washed array was transferred to a new 10 cm dish filled with pre-warmed differentiation medium composed of DMEM/F12, 10% BIT9500 (Stem Cell Technologies), 0.2 μM all-*trans* retinoic acid (Sigma), 10 ng/ml of NT3 and BDNF (Peprotech), and twice the recommended dose of penicillin, streptomycin, and fungizone (Gibco). Medium was replaced with fresh differentiation medium within 12–15 h from plating. Arrays were cultured for periods ranging from 1 to 4 days. BrdU (2 μM final concentration) was added 12–13 h prior to the end of the experiment.

Immunostaining

Cells were fixed with 4% PFA for 15 min at 4°C, washed with CMF PBS, and blocked for 30 min with 3% donkey serum (Jackson) and 0.3% Triton X-100 (Fisher) in TBS. Arrays were incubated overnight at 4°C with rabbit anti-beta-tubulin III (TUJ1, Covance) and guinea-pig anti-GFAP (Advanced ImmunoChemical Inc.). Following 3 × wash with TBS, arrays were incubated for 3 h (room temperature) with FITC-conjugated donkey anti-rabbit IgG (Jackson ImmunoResearch) and Cy5-conjugated donkey anti-guinea-pig IgG (Jackson Immuno Research). Arrays were washed 3 × and fixed again with 4% PFA, followed by washing. To uncover the BrdU epitope, the arrays were treated with 2 N HCl for 16 min at 37°C. To stain for BrdU incorporation, the slides were blocked, incubated overnight with rat anti-BrdU (Accurate Chemical & Scientific Corporation), washed 3 ×, and incubated with Cy3-conjugated donkey anti-rat IgG (Jackson ImmunoResearch) for 3 h. Arrays were then washed and stained with DAPI for 2 min. Counterstained arrays were mounted with a coverslip gapped by 100 μl of 2.5% DAPCO-PVA solution and stored at 4°C for 2 days prior to imaging. Examination of arrays prior and following staining showed that there were no relative cell detachments.

Imaging and feature extraction

Counterstained arrays were imaged through the coverslip using a fully automated fluorescence microscopy system (*ImageXpress*, Axon Instruments). Imaging was controlled through an acquisition script that runs within the ImageXpress software environment. The system was programmed to visit each spot on the array, perform (wavelength-dependent) autofocus, and uniformly acquire 20 × DAPI, FITC (TUJ1), Cy3 (BrdU), and Cy5 (GFAP) images. Four-channel images were annotated with imaging- and experimental-related information and stored as frames of four, 16-bit Tiff images in a built-in image database. Feature extraction was performed using analysis scripts that employ built-in segmentation algorithms. The nuclei of all the cells in a spot were detected using blob detection in the DAPI channel followed by measurements of nucleus area and aspect ratio. Proliferating cells were identified based on BrdU threshold crossing and the replication index was defined as the ratio between the number of BrdU-positive nuclei and the total number of cells. Cells were classified into neurons and glia based on TUJ1 and GFAP intensities in a narrow ring (0.55 μm in width) surrounding each nucleus. Perinuclear rings satisfying the dual requirement of low TUJ1 intensity and medium to high GFAP intensity were declared as belonging to glial cells and vice versa for neurons. Percentages of differentiating neurons and glial cells (Figure 3A) were obtained by dividing the number of identified neurons (glia) by the total number of cells. A gliogenic (g/n) index was defined as the ratio between the number of glial and neuronal cells. Normalized glia to neural ratio (Figure 3B) was obtained by dividing the gliogenic index by the average inter-nuclear distance. The perinuclear intensities were also used to analyze the extent of differentiation in individual cells. 'Direction' of differentiation was defined as the ratio of GFAP and TUJ1 intensities in the same cell. 'Extent' of differentiation was defined as the square root of the sum of the squares of GFAP and TUJ1 intensities, computed for each cell individually. Ensemble average values for the direction and extent of differentiation were obtained by averaging over all the cells that were exposed to the same spot composition.

Data analysis

Ensemble average phenotypes representing distinct signaling compositions were obtained by averaging single cell measurements across spots of identical signaling composition. Maps connecting external stimulation and (ensemble average) cellular properties were represented by matrices, with rows and columns corresponding to signaling combinations and phenotypes, respectively. All rows were normalized (term by term) either by the Ln phenotypes (Figure 5A and Supplementary Figure S5A) or by the phenotypes measured for one of three co-signals (Supplementary Figure S6). Normalized values were log-scaled (base 2) and columns were scaled to a unit standard deviation. Rows and columns were (hierarchically) clustered using *Acuity* software (Axon Instruments) with Pearson correlation as the similarity metric.

Each signaling combination was associated with a response magnitude (Supplementary Figure S5A) defined with respect to a given parameter set as follows: measured parameters were divided

by the corresponding values on Ln alone, and absolute values of log-scaled ratios (base 2) were averaged across all the parameters in the set.

Dominance over individual parameters (or the response magnitude) was defined as follows: for each parameter measured Y and a pair of signals A and B, the dominance of A over B with respect to Y was defined by $D_Y(A;B)=[|Y_{A+B}-Y_B|-|Y_{A+B}-Y_A|]/|Y_{A+B}|$.

Supplementary information

Supplementary information is available at the *Molecular Systems Biology* website (www.nature.com/msb).

Acknowledgements

References

Al-Hajj M, Wicha MS, Benito-Hernandez A, Morrison SJ, Clarke MF (2003) Prospective identification of tumorigenic breast cancer cells. *Proc Natl Acad Sci USA* **100:** 3983–3988

Anderson DG, Levenberg S, Langer R (2004) Nanoliter-scale synthesis of arrayed biomaterials and application to human embryonic stem cells. *Nat Biotechnol* **22:** 863–866

Anderson DJ (2001) Stem cells and pattern formation in the nervous system: the possible versus the actual. *Neuron* **30:** 19–35

Bailey SN, Sabatini DM, Stockwell BR (2004) Microarrays of small molecules embedded in biodegradable polymers for use in mammalian cell-based screens. *Proc Natl Acad Sci USA* **101:** 16144–16149

Bertrand N, Castro DS, Guillemont F (2002) Proneural genes and the specification of neuronal cell types. *Nat Rev Neurosci* **3:** 517–530

Caccamo DV, Herman MM, Frankfurter A, Katsetos CD, Collins VP, Rubinstein LJ (1989) An immunohistochemical study of neuropeptides and neuronal cytoskeletal proteins in the neuroepithelial component of a spontaneous murine ovarian teratoma. Primitive neuroepithelium displays immunoreactivity for neuropeptides and neuron-associated beta-tubulin isotype. *Am J Pathol* **135:** 801–813

Chen DS, Soen Y, Stuge TB, Lee PP, Weber JS, Brown PO, Davis MM (2005) Marked differences in human melanoma antigen-specific T cell responsiveness after vaccination using a functional microarray. *PLoS Med* **2:** 1018–1030

Duncan AW, Rattis FM, DiMascio LN, Congdon KL, Pazianos G, Zhao C, Yoon K, Cook JM, Willert K, Gaiano N, Reya T (2005) Integration of Notch and Wnt signaling in hematopoietic stem cell maintenance. *Nat Immunol* **6:** 314–322

Easter Jr SS, Ross LS, Frankfurter A (1993) Initial tract formation in the mouse brain. *J Neurosci* **13:** 285–299

Edlund T, Jessell TM (1999) Progression from extrinsic to intrinsic signaling in cell fate specification: a view from the nervous system. *Cell* **96:** 211–224

Eisen MB, Spellman PT, Brown PO, Botstein D (1998) Cluster analysis and display of genome-wide expression patterns. *Proc Natl Acad Sci USA* **95:** 14863–14868

Flaim CJ, Chien S, Bhatia SN (2005) An extracellular matrix microarray for probing cellular differentiation. *Nat Methods* **2:** 119–125

Gaiano N, Fishell G (2002) The role of Notch in promoting glial and neural stem cell fates. *Annu Rev Neurosci* **25:** 471–490

Gaiano N, Nye JS, Fishell G (2000) Radial glial identity is promoted by Notch1 signaling in the murine forebrain. *Neuron* **26:** 395–404

Gajavelli S, Wood PM, Pennica D, Whittemore SR, Tsoulfas P (2004) BMP signaling initiates a neural crest differentiation program in embryonic rat CNS stem cells. *Exp Neurol* **188:** 205–223

Ge W, Martinowich K, Wu X, He F, Miyamoto A, Fan G, Weinmaster G, Sun YE (2002) Notch signaling promotes astrogliogenesis via direct CSL-mediated glial gene activation. *J Neurosci Res* **69:** 848–860

Gross RE, Mehler MF, Mabie PC, Zang Z, Santschi L, Kessler JA (1996) Bone morphogenetic proteins promote astroglial lineage commitment by mammalian subventricular zone progenitor cells. *Neuron* **17:** 595–606

Hogg RC, Chipperfield H, Whyte KA, Stafford MR, Hansen MA, Cool SM, Nurcombe V, Adams DJ (2004) Functional maturation of isolated neural progenitor cells from the adult rat hippocampus. *Eur J Neurosci* **19:** 2410–2420

Jessell TM (2000) Neuronal specification in the spinal cord: inductive signals and transcriptional codes. *Nat Rev Genet* **1:** 20–29

Johe KK, Hazel TG, Muller T, Dugich-Djordjevic MM, McKay RD (1996) Single factors direct the differentiation of stem cells from the fetal and adult central nervous system. *Genes Dev* **10:** 3129–3140

Lee MK, Tuttle JB, Rebhun LI, Cleveland DW, Frankfurter A (1990) The expression and posttranslational modification of a neuron-specific beta-tubulin isotype during chick embryogenesis. *Cell Motil Cytoskeleton* **17:** 118–132

Li W, Cogswell CA, LoTurco JJ (1998) Neuronal differentiation of precursors in the neocortical ventricular zone is triggered by BMP. *J Neurosci* **18:** 8853–8862

Lie DC, Dziewczapolski G, Willhoite AR, Kaspar BK, Shults CW, Gage FH (2002) The adult substantia nigra contains progenitor cells with neurogenic potential. *J Neurosci* **22:** 6639–6649

Morrison SJ, Perez SE, Qiao Z, Verdi JM, Hicks C, Weinmaster G, Anderson DJ (2000) Transient Notch activation initiates an irreversible switch from neurogenesis to gliogenesis by neural crest stem cells. *Cell* **101:** 499–510

Morrison SJ, Shah NM, Anderson DJ (1997) Regulatory mechanisms in stem cell biology. *Cell* **88:** 287–298

Palmer TD, Schwartz PH, Taupin P, Kaspar B, Stein SA, Gage FH (2001) Cell culture: Progenitor cell from human brain after death. *Nature* **411:** 42–43

Park JK, Williams BP, Alberta JA, Stiles CD (1999) Bipotent cortical progenitor cells process conflicting cues for neurons and glia in a hierarchical manner. *J Neurosci* **19:** 10383–10389

Pixley SK, de Vellis J (1984) Transition between immature radial glia and mature astrocytes studied with a monoclonal antibody to vimentin. *Brain Res* **317:** 201–209

Ross SE, Greenberg ME, Stiles CD (2003) Basic helix–loop–helix factors in cortical development. *Neuron* **39:** 13–25

Sauvageot CM, Stiles CD (2002) Molecular mechanisms controlling cortical gliogenesis. *Curr Opin Neurobiol* **12:** 244–249

Schwartz PH, Bryant PJ, Fuja TJ, Su H, O'Dowd DK, Klassen H (2003) Isolation and characterization of neural progenitor cells from post-mortem human cortex. *J Neurosci Res* **74:** 838–851

Shah NM, Anderson DJ (1997) Integration of multiple instructive cues by neural crest stem cells reveals cell-intrinsic biases in relative growth factor responsiveness. *Proc Natl Acad Sci USA* **94:** 11369–11374

Shah NM, Groves AK, Anderson DJ (1996) Alternative neural crest cell fates are instructively promoted by TGFbeta superfamily members. *Cell* **85:** 331–343

Shah NM, Marchionni MA, Isaacs I, Stroobant P, Anderson DJ (1994) Glial growth factor restricts mammalian neural crest stem cells to a glial fate. *Cell* **77:** 349–360

Soen Y, Chen DS, Kraft DL, Davis MM, Brown PO (2003) Detection and characterization of cellular immune responses using peptide-MHC microarrays. *PLoS Biol* **1:** 429–438

Song H, Stevens CF, Gage FH (2002) Astroglia induce neurogenesis from adult neural stem cells. *Nature* **417:** 39–44

Sun Y, Nadal-Vicens M, Misono S, Lin MZ, Zubiaga A, Hua X, Fan G, Greenberg ME (2001) Neurogenin promotes neurogenesis and inhibits glial differentiation by independent mechanisms. *Cell* **104:** 365–376

Sun YE, Martinowich K, Ge W (2003) Making and repairing the mammalian brain—signaling towards neurogenesis and gliogenesis. *Semin Cell Dev Biol* **14:** 161–168

Temple S (2001) The development of neural stem cells. *Nature* **414:** 112–117

van Praag H, Schinder AF, Christie BR, Toni N, Palmer TD, Gage FH (2002) Functional neurogenesis in the adult hippocampus. *Nature* **415:** 1030–1034

Varnum-Finney B, Wu L, Yu M, Brashem-Stein C, Staats S, Flowers D, Griffin JD, Bernstein ID (2000) Immobilization of Notch ligand, Delta-1, is required for induction of Notch signaling. *J Cell Sci* **113:** 4313–4318

Wang S, Barres BA (2000) Up a Notch: instructing gliogenesis. *Neuron* **27:** 197–200

Wheeler DB, Bailey SN, Guertin DA, Carpenter AE, Higgins CO, Sabatini DM (2004) RNAi living-cell microarrays for loss-of-function screens in *Drosophila melanogaster* cells. *Nat Methods* **1:** 127–132

Wofchuck ST, Rodnight R (1995) Age-dependent changes in the regulation by external calcium ions of the phosphorylation of glial fibrillary acidic protein in slices of rat hippocampus. *Brain Res Dev Brain Res* **85:** 181–186

Ziauddin J, Sabatini DM (2001) Microarrays of cells expressing defined cDNAs. *Nature* **411:** 107–110